Electronic Supplementary Material (ESI) for Energy & Environmental Science.

Perovskite-silicon tandem solar modules with optimised light harvesting

Manoj Jaysankar, Miha Filipič, Bartosz Zielinski, Raphael Schmager, Wenya Song, Weiming Qiu, Ulrich W. Paetzold, Tom Aernouts, Maarten Debucquoy, Robert Gehlhaar, and Jef Poortmans

Supporting Information

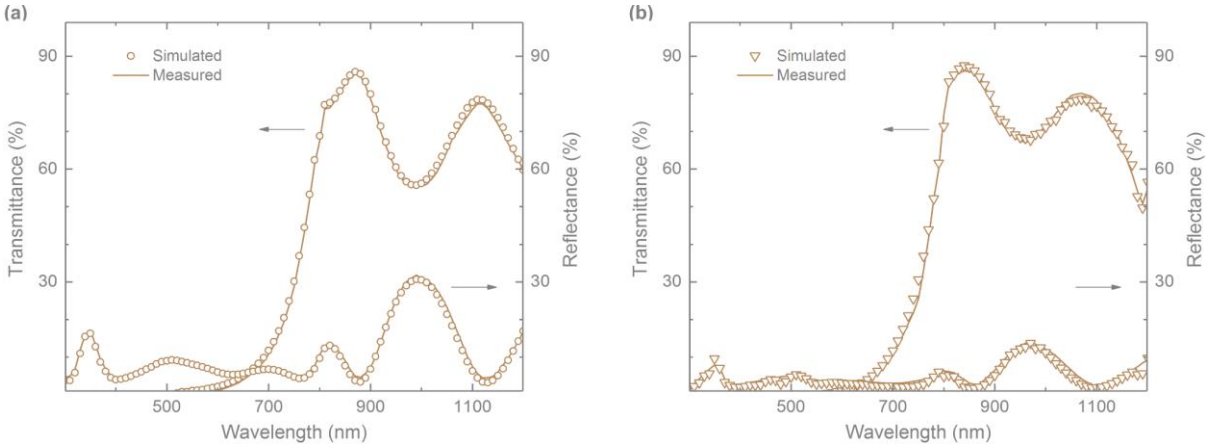

Figure S1: Simulated and measured transmittance, reflectance spectra of semi-transparent perovskite solar cell **(a)** without textured film and **(b)** with textured film. The spectra of solar cells and solar modules are identical.

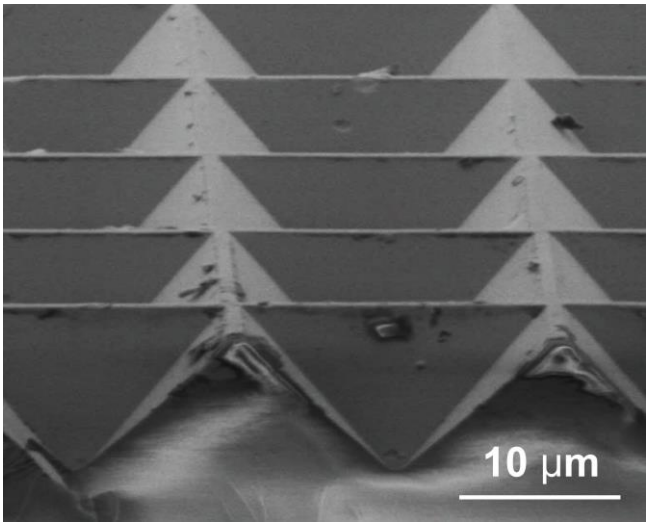

Figure S2: Scanning electron microscopy image of the textured film with inverted pyramids.

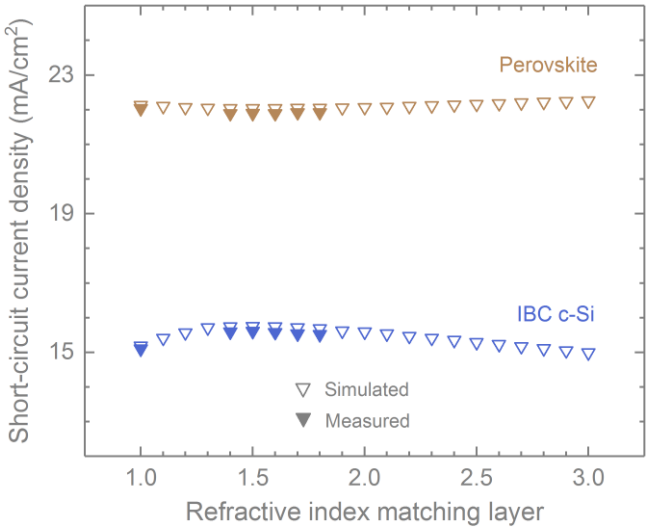

Figure S3: Effect of refractive index of the index matching layer on short-circuit current density of perovskite top solar cell and IBC c-Si bottom solar cell with optimised textured film.

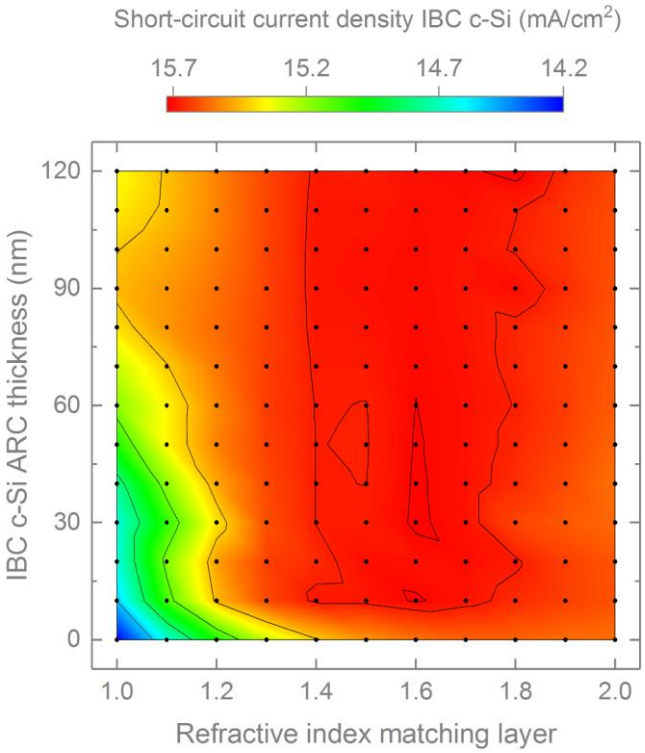

Figure S4: Effect of refractive index of index matching layer and thickness of IBC c-Si anti-reflective coating (ARC) on short-circuit current density of IBC c-Si bottom solar cell in tandem configuration with optimally textured perovskite top solar cell.

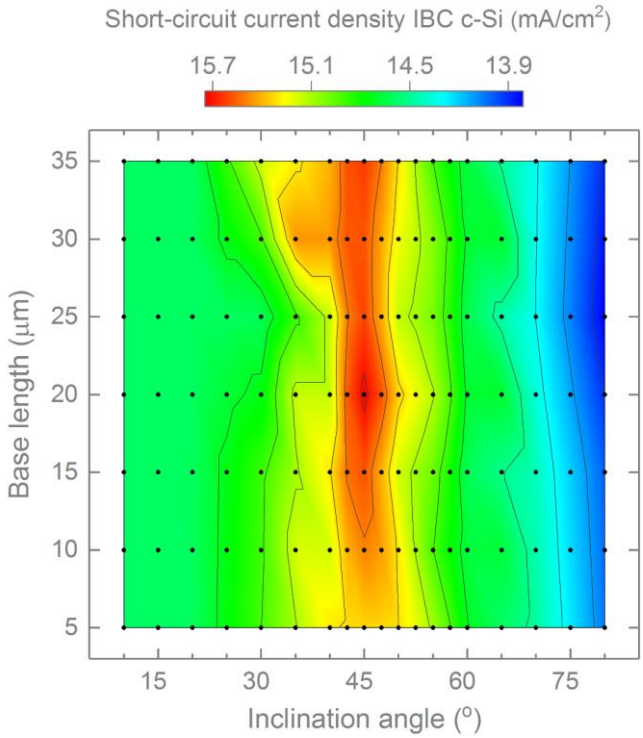

Figure S5: Impact of inclination angle and base length of inverted pyramidal texture on short-circuit current density of IBC c-Si bottom solar cell with an index matching layer of refractive index 1.5.

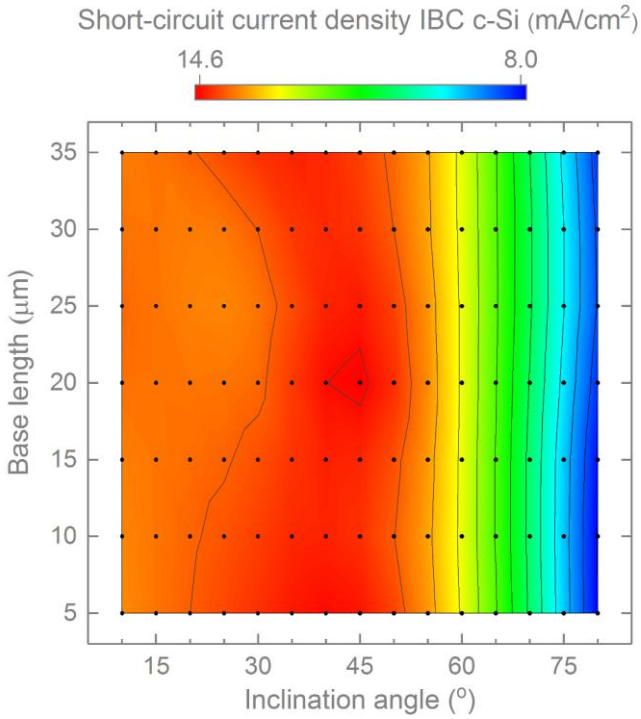

Figure S6: Impact of inclination angle and base length of upright pyramidal textures on short-circuit current density (J_{SC}) of IBC c-Si bottom solar cell. Using upright pyramids results in a peak J_{SC} of 14.6 mA/cm^2, which is lower than the 15.1 mA/cm^2 for inverted pyramids. The intermediate medium between top and bottom solar cells is air.

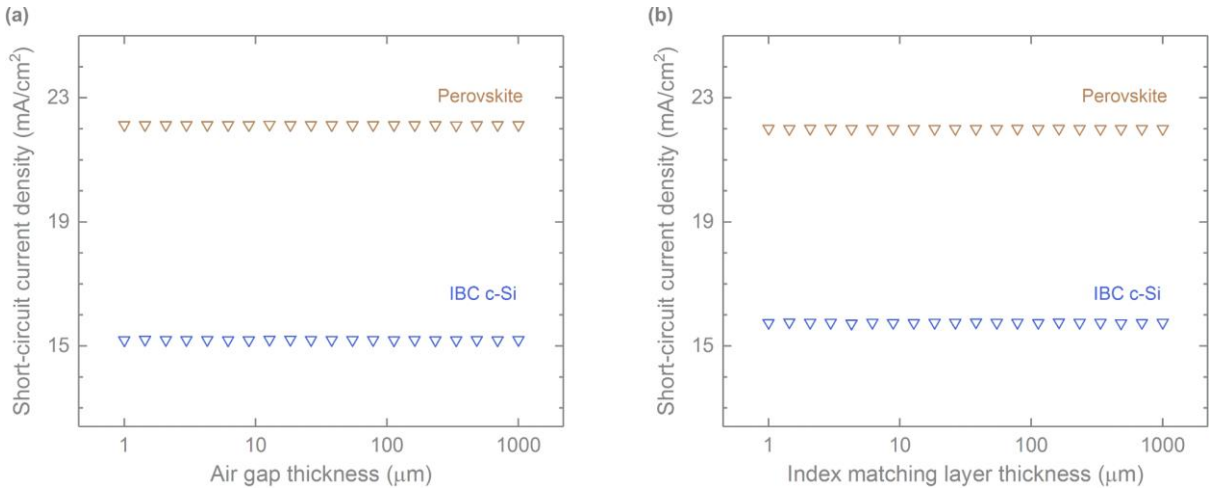

Figure S7: Influence of thickness of **(a)** air gap and **(b)** refractive index matching layer on the short-circuit current density of the perovskite and IBC c-Si solar cells.

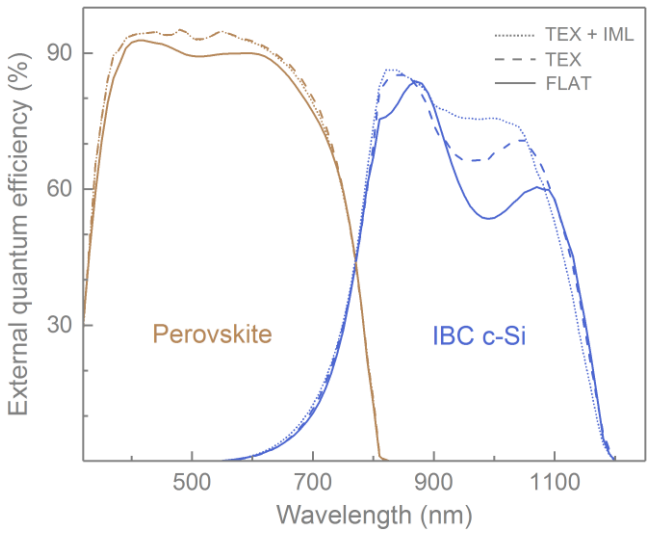

Figure S8: Simulated external quantum efficiency of perovskite top solar cell and IBC c-Si bottom solar cell in tandem configuration in three different cases.

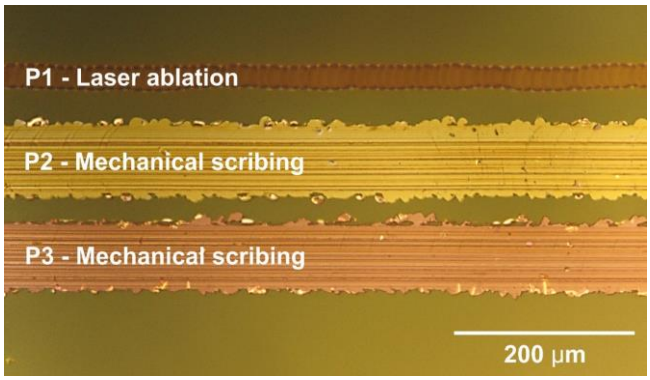

Figure S9: Optical microscopy image of P1, P2, and P3 scribes of the perovskite solar module.

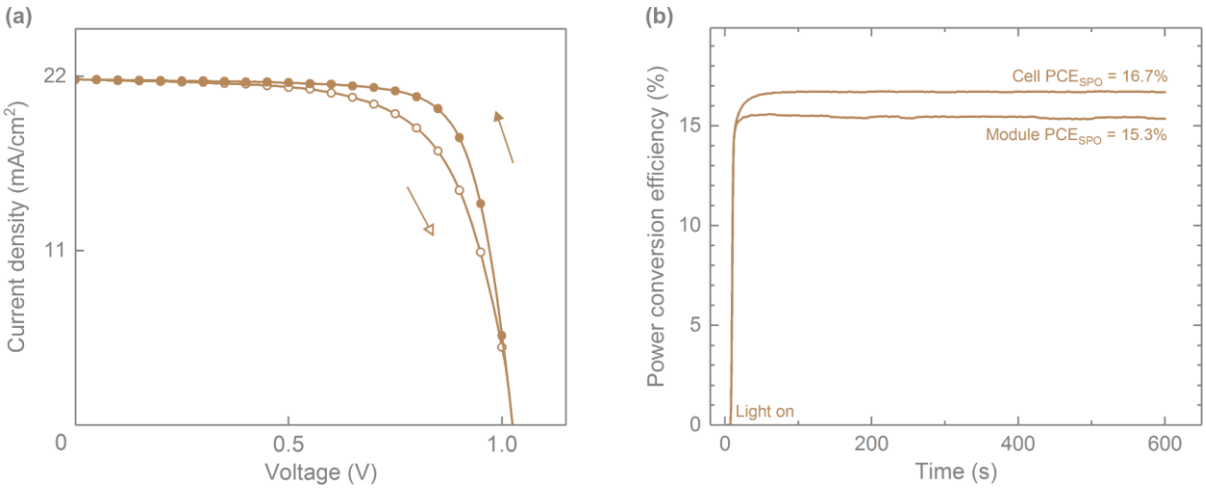

Figure S10: (a) Measured hysteresis scan of stand-alone semi-transparent perovskite solar cell. Semi-transparent perovskite solar module also shows similar hysteresis behavior. **(b)** The semi-transparent perovskite solar cells and modules show stable power output (PCE_{SPO}) during operation at maximum power point.

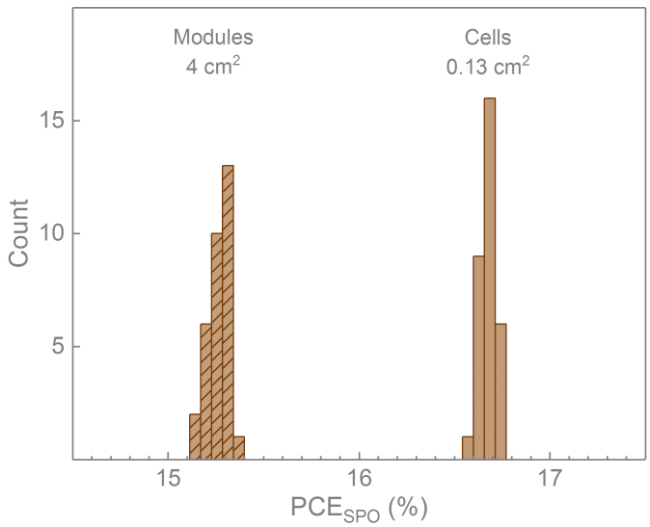

Figure S11: Histogram representing the spread in stabilized power output (PCE_{SPO}) of semi-transparent perovskite solar cells and modules.

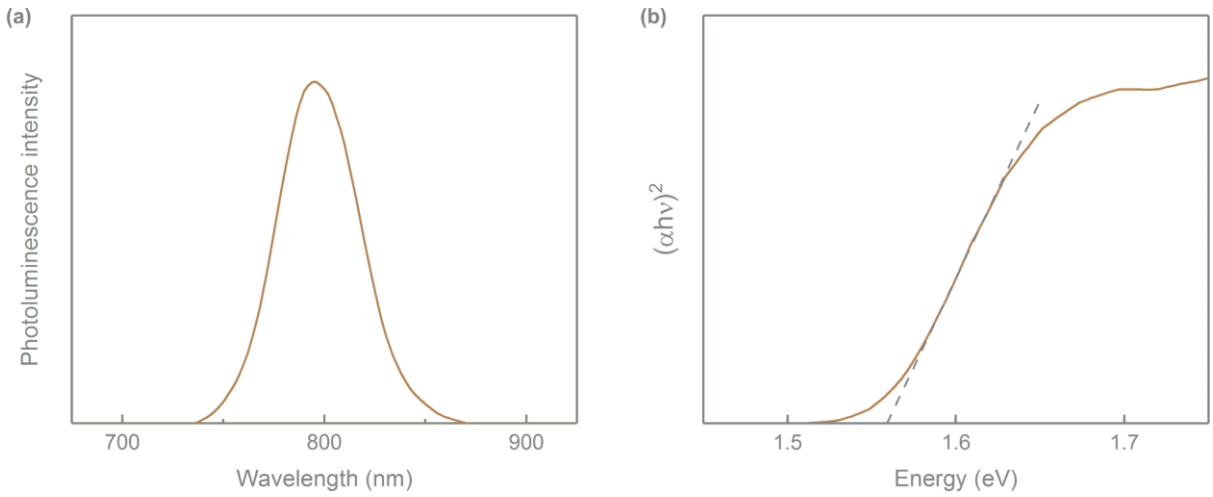

Figure S12: (a) Measured photoluminescence spectrum and **(b)** Tauc plot of the perovskite absorber. The extracted bandgap is 1.56 eV.

Table S1: Optical analysis of Perovskite-IBC c-Si tandem stack in the reference case (FLAT) and the case with optimised textured film and refractive index matching layer of refractive index 1.5 (TEX + IML). The photocurrent density attributable to various processes was integrated for wavelengths from 300 nm to 1200 nm assuming AM 1.5G irradiance.

	Integrated photocurrent density in mA/cm²			
	FLAT		**TEX + IML**	
Overall reflection	5.87	(12.7%)	2.20	(4.8%)
Absorption in glue	-		0.32	(0.7%)
Absorption in glass	1.63	(3.5%)	1.86	(4.0%)
Absorption in ITO (front)	1.86	(4.0%)	2.44	(5.3%)
Absorption in TiO_2	0.04	(0.1%)	0.04	(0.1%)
Absorption in CsFAPbIBr	21.40	(46.3%)	22.09	(47.8%)
Absorption in Spiro-OMeTAD	0.43	(0.9%)	0.54	(1.2%)
Absorption in ITO (rear)	0.11	(0.2%)	0.14	(0.3%)
Absorption in c-Si	14.15	(30.6%)	15.86	(34.3%)
Absorption in c-Si rear contacts	0.77	(1.7%)	0.77	(1.7%)

Table S2: Simulated short-circuit current density (J_{SC}) of IBC c-Si bottom solar cell for different index matching layers and anti-reflective coating (ARC) thicknesses.

Case	Index matching layer refractive index	IBC c-Si ARC thickness (nm)	J_{SC} of IBC c-Si (mA/cm^2)
TEX	1.0	60	15.19
TEX + IML	1.5	60	15.70
Optimal	1.6	40	15.74

Table S3: Average values of photovoltaic parameters of semi-transparent perovskite solar cell (0.13 cm^2) and IBC c-Si solar cell (4 cm^2) measured under 1000 W/m^2 AM 1.5G irradiance. The response of the IBC c-Si solar cell in four-terminal configuration is measured with the incident light filtered through a 4 cm^2 semi-transparent perovskite solar module. The reported power conversion efficiencies are stabilised power outputs (PCE_{SPO}) tracked at maximum power point for 10 minutes.

	Device	J_{SC} (mA/cm^2)	V_{OC} (V)	FF (%)	Aperture PCE_{SPO} (%)
Stand alone	Perovskite	21.8 ± 0.1	1.02 ± 0.02	73.7 ± 1.4	16.7 ± 0.3
	IBC c-Si	41.3 ± 0.04	0.691 ± 0.001	80.6 ± 0.1	23.0 ± 0.01
FLAT	Perovskite	21.8 ± 0.1	1.02 ± 0.02	73.6 ± 1.4	16.7 ± 0.3
	IBC c-Si	14.1 ± 0.06	0.673 ± 0.002	81.7 ± 0.1	7.8 ± 0.02
	Tandem				24.5 ± 0.3
TEX	Perovskite	22.0 ± 0.1	1.02 ± 0.01	73.6 ± 1.4	16.8 ± 0.2
	IBC c-Si	15.1 ± 0.01	0.674 ± 0.001	81.7 ± 0.1	8.3 ± 0.04
	Tandem				25.1 ± 0.2
TEX + IML	Perovskite	22.0 ± 0.1	1.01 ± 0.02	73.4 ± 1.3	16.7 ± 0.3
	IBC c-Si	15.6 ± 0.03	0.674 ± 0.002	81.7 ± 0.1	8.6 ± 0.04
	Tandem				25.3 ± 0.3